Proc. Estonian Acad. Sci. Phys. Math., 1994, 43, 2, 102 – 117
https://doi.org/10.3176/phys.math.1994.2.06

A QUASIGEOSTROPHIC MODEL WITH TEMPERATURE AND GROUND SURFACE PRESSURE IN THE ROLE OF BASIC FIELDS

Rein RÕÕM

Astrofüüsika ja Atmosfäärifüüsika Instituut (Institute of Astrophysics and Atmospheric Physics), EE-2444 Tôravere, Eesti (Estonia)

Presented by A. Sapar

Received December 9, 1993; accepted April 6, 1994

Abstract. A quasigeostrophic model is derived, including the ground surface pressure tendency equation along with the temperature equation as main prognostic equations. The model is completed by the omega-equation with non-homogeneous boundary conditions. The obtained model incorporates features of both the ordinary quasigeostrophic model for thermally stratified fluid and the shallow-water barotropic model. The simplest realization of the obtained equations is a one-level baroclinic model where temperature fluctuations are height-independent. As examples of numeric integration show, the one-level model is capable of a qualitatively adequate description of polar front evolution and accompanying formation of highs and lows in the lower troposphere.

Key words: quasigeostrophic equations, temperature, ground surface pressure.

1. INTRODUCTION

Though most of recent quantitative results on atmospheric circulation have been obtained using the full system of primitive equations, filtered equations, i.e. the models where acoustic and buoyancy waves have been filtered, have not lost their significance. Main advantage of the filtered equations is that they, being essentially more simple in treatment than primitive equations, provide a qualitatively true description of key processes in the atmosphere. The most common in the family of filtered equations is the quasigeostrophic (QG) model, the primary ideas of which were outlined in [1–4]. A profound treatment of the origin and nature of the QG model is presented in [5].

The shortcoming of the QG model is that it does not provide quantitatively reasonable forecasts. This has been the main reason for numerous efforts to improve the QG model and develop filtered equations, which are more general, use less restrictive assumptions and at the same

time still retain simplicity. The development has been proceeded in two main directions: 1) by incorporating into filtered equations terms proportional to the second and higher powers of the Rossby number; 2) by making transformations to special co-ordinate sets. The classical generalization of the QG model is the semigeostrophic model [6]. In recent years a number of filtered equations, called intermediate models, have been described for the baroclinic atmosphere by [7], and for the barotropic shallow-water case by [8].

As it turns out, the classical common QG model (and all the truncated models of the second generation) employ along with the quasigeostrophic assumption, which enables an approximate solution of the equation of mechanical motion, another approximation, which may be called (using an analogy with ocean dynamics) the rigid bottom approximation. This approximation arises as a result of the use of the zero condition for the vertical velocity at the lower boundary in the baric co-ordinate space. Though valid in the shorter synoptic-scale domain of motions, the rigid bottom approximation is not a neccessary part of the QG framework and its application involves no simplifications in the model.

In this paper we will propose a complete quasigeostrophic model, which does not apply the rigid bottom approximation and which incorporates in full length all effects connected with the free boundary of the atmosphere in pressure co-ordinates. As a result, a simple clear QG approach will be created, which uses temperature and ground surface pressure (GSP) as basic prognostic fields. The model is valid in the broad range of synoptic and planetary scale motions. The common QG model and the shallow-water model can be derived from it as special cases.

2. DECOMPOSITION OF THE GEOPOTENTIAL

In this paper the baric co-ordinates $\mathbf{x}$, p are used, where $\mathbf{x} = (x, y)$ present "horizontal" co-ordinates and the pressure p is the vertical co-ordinate.

The total geopotential is in pressure co-ordinates

$$\tilde{\Phi}(\mathbf{x}, p, t) = gZ(\mathbf{x}) + R\int_{p}^{p_s(x,t)} \frac{\tilde{T}(\mathbf{x}, p', t)}{p'} \mathrm{d}p',$$

where Z presents the height of the ground surface above the sea-level, p_S is the actual pressure at the ground and $\tilde{T}$ is the total temperature. For the following treatment it is convenient to decompose the total geopotential as a sum of the main component and thermal and baric fluctuations. For that we present $\tilde{T}$ as a sum

$$\tilde{T}(\mathbf{x}, p, t) = T_0(p) + T(\mathbf{x}, p, t),$$

where T_0 is an appropriately chosen profile of the mean temperature. As a consequence, the geopotential can be expanded as

$$\tilde{\Phi}(\mathbf{x}, p, t) = \Phi_0(p) + \Phi_T(\mathbf{x}, p, t) + \Phi_b(\mathbf{x}, t). \quad (2.1)$$

Here

$$\Phi_0(p) = gZ(\mathbf{x}) + R\int_p^{p_0(\mathbf{x})} \frac{T_0(p')}{p'} dp' \quad (2.2)$$

is the mean component of the geopotential which does not depend on the horizontal co-ordinates $\mathbf{x}$ and the time t due to the use of the balanced value for the mean ground surface pressure field

$$p_0(\mathbf{x}) = a \exp\left\{-\frac{g}{R}\int_0^{Z(\mathbf{x})} \frac{dz'}{T_0}\right\}, \quad (2.3)$$

a being the mean GSP at the sea-level. The componets Φ_T and Φ_b present the thermally and barically forced fluctuations of the geopotential at the pressure level p:

$$\Phi_T(\mathbf{x}, p, t) = R\int_p^{p_s(\mathbf{x}, t)} \frac{T(\mathbf{x}, p', t)}{p'} dp', \quad (2.4)$$

$$\Phi_b(\mathbf{x}, t) = R\int_{p_0(\mathbf{x})}^{p_s(\mathbf{x}, t)} \frac{T_0(p')}{p'} dp'. \quad (2.5)$$

The presentation of the geopotential by formulae (2.1)–(2.5) is exact, no limiting assumptions or approximations are used here. Meanwhile, in practice, using the smallness of the pressure fluctuation at the ground

$$\xi = p_s - p_0,$$

thermal and baric components of the geopotential can be approximated with a good accuracy as

$$\Phi_T(\mathbf{x}, p, t) \approx R\int_p^{p_0(\mathbf{x})} \frac{T(\mathbf{x}, p', t)}{p'} dp', \quad (2.4a)$$

$$\Phi_b(\mathbf{x}, t) \approx c_e^2 \frac{\xi}{p_0}, \quad (2.5a)$$

where

$$c_e = \sqrt{RT_0[p_0(\mathbf{x})]}$$

is the speed of external buoyancy waves. The approximations used cause an error in the horizontal pressure force, which does not exceed a few per cent, and they are applicable both for primitive equations and for the QG model. The approximation of thermal and baric geopotentials by formulae (2.4a) and (2.5a) must be accompanied by the replacement of the inital domain occupied by the atmosphere in the p-space

$$0 \le p \le p_s(\mathbf{x}, t), \quad (2.6)$$

by the domain

$$0 \le p \le p_0(\mathbf{x}). \tag{2.6a}$$

In the approximated case the thermal geopotential Φ_T becomes zero at the mean lower boundary $p = p_0$ according to (2.4a). Meanwhile, the fluctuative part of the geopotential is not zero at this level:

$$\left(\tilde{\Phi} - \Phi_0\right)_{p=p_0} = \Phi_b.$$

Thus Φ_b, which, according to (2.5a), is proportional to the fluctuation of the free surface in pressure co-ordinates from the mean value, determines approximately the fluctuative part of the geopotential at the mean GSP level.

The horizontal pressure force is caused entirely by the baric and thermal fluctuations Φ_b and Φ_T. The interference of these two fields causes all the diversity of the vertical structure of cyclones and anticyclones including such characteristic features of baric systems as tilting of axes of cyclones and anticyclones, weakening and disappearing of surface highs and lows with height, conversion of a mid-tropospheric thermal low into the baric high at the ground, etc. The significance of expansion (2.1) is that it moves to the foreground the role of the ground GSP fluctuations in atmospheric processes. Using presentation (2.1), the problem of the dynamics of the fields T and ξ arises.

3. THE QUASIGEOSTROPHIC MODEL IN VARIABLES TEMPERATURE – GSP FLUCTUATION

We will apply the beta-plane approximation for the Coriolis parameter

$$f = f_0 + \beta \cdot (y - y_0), \quad \beta = (\partial f/\partial y)_{y_0},$$

and consider the atmosphere above the flat ground in pressure co-ordinates

$$0 < p < p_0 = a.$$

Application of quasigeostrophic assumptions to the full set of primitive equations [9, 10] in the pressure co-ordinates leads to prognostic equations for T and ξ

$$\frac{\mathrm{d}_g}{\mathrm{d}t} T = T_i \frac{\omega}{p} + W/c_p, \tag{3.1}$$

$$\frac{\overline{\mathrm{d}}_g}{\mathrm{d}t} \xi = \omega_s, \tag{3.2}$$

where $\mathrm{d}_g/\mathrm{d}t$ and $\overline{\mathrm{d}}_g/\mathrm{d}t$ are geostrophic total derivatives

$$\frac{\mathrm{d}_g}{\mathrm{d}t} = \frac{\partial}{\partial t} + \mathbf{v}_g \nabla, \quad \frac{\overline{\mathrm{d}}_g}{\mathrm{d}t} = \frac{\partial}{\partial t} + \bar{\mathbf{v}}_g \nabla, \tag{3.3}$$

and the overbar denotes vertical averaging

$$\overline{(\ldots\ldots)} = \frac{1}{a}\int_0^a (\ldots\ldots)\,\mathrm{d}p.$$

W is the heating rate per unit mass, c_p – the gas constant. The reference temperature

$$T_i(p) = \frac{R}{c_p}T_0(p) - p\frac{\mathrm{d}T_0}{\mathrm{d}p} = -T_0\frac{p}{\theta_0}\frac{\mathrm{d}\theta_0}{\mathrm{d}p} > 0, \tag{3.4}$$

where θ_0 is the mean potential temperature, presents the basic stability parameter of the mean atmosphere. The following relation holds between T_i and the stability parameter σ used in [9]: $T_i = p^2\sigma\ /R$. The vertical velocity $\omega = \mathrm{d}p/\mathrm{d}t$ is determined by horizontal wind as

$$\omega(\mathbf{x}, p, t) = -\int_0^p \mathrm{div}\,\mathbf{v}(\mathbf{x}, p', t)\,\mathrm{d}p', \quad \omega_s = \omega|_{p=a}, \tag{3.5}$$

and the wind velocity is

$$\mathbf{v} = \mathbf{v}_g + \mathbf{v}_a, \tag{3.6}$$

where geostrophic and ageostrophic components are determined by relations

$$f_0\mathbf{e}_v \times \mathbf{v}_g = -\nabla\,(\Phi_T + \Phi_b), \tag{3.7a}$$

$$f_0\mathbf{e}_v \times \mathbf{v}_a = -\frac{\mathrm{d}_g}{\mathrm{d}t}\mathbf{v}_g - \beta\cdot(y - y_0)\,\mathbf{e}_v \times \mathbf{v}_g + \mathbf{F}. \tag{3.7b}$$

Here $\mathbf{F}$ presents the turbulent friction force.

Since prognostic Eqs. (3.1) and (3.2) include besides temperature and GSP advections the vertical velocity ω, it is convenient to apply Eqs. (3.1) and (3.2) along with the omega-equation which in case of relations (3.1)–(3.7) is

$$\left(p\frac{\partial^2}{\partial p^2}p + l_i^2\Delta\right)\frac{\omega}{p} = -S, \tag{3.8a}$$

$$\left(\frac{\partial\omega}{\partial p} - l_e^2\Delta\frac{\omega}{p}\right)_{p=a} = \sigma, \tag{3.8b}$$

$$\omega|_{p=0} = 0. \tag{3.8c}$$

$$S = \frac{p}{f_0}\frac{\partial}{\partial p}(A_\eta + \mathbf{e}_v\mathrm{rot}\,\mathbf{F}) + \frac{R}{f_0^2}\Delta\,(A_T + W/c_p), \tag{3.9}$$

$$\sigma = \frac{l_e^2}{a}\Delta A_\xi - \frac{1}{f_0}(A_\eta + \mathbf{e}_v\mathrm{rot}\,\mathbf{F})_{p=a}. \tag{3.10}$$

Here $\Delta = \nabla^2$,

$$l_e = \sqrt{RT_0(a)}/f_0, \quad l_i = \sqrt{RT_i(p)}/f_0$$

are the external and internal Rossby deformation radii, A_T and A_ξ are the geostrophic advections of temperature and GSP fluctuations

$$A_T = -\mathbf{v}_g \nabla T, \quad A_\xi = -\bar{\mathbf{v}}_g \nabla \xi, \tag{3.11a}$$

$\mathbf{e}_v$ is the vertical unit vector, and

$$A_\eta = -\mathbf{v}_g \nabla \eta \tag{3.11b}$$

is the advection of the geostrophic absolute vorticity

$$\eta = \frac{1}{f_0} \nabla (\Phi_b + \Phi_T) + f. \tag{3.12}$$

Eq. (3.8a) and the boundary condition (3.8b) are exact and no simplifications are made at their founding. They are derived from the condition of the coincidence of two various prognostic equations for the absolute vorticity η. An equation for the absolute vorticity follows from the ageostrophic relation (3.7b) after acting with the operator $\mathbf{e}_v$rot and it has the form of the common QG vorticity equation

$$\frac{\mathrm{d}_g}{\mathrm{d}t}\eta = f_0 \frac{\partial \omega}{\partial p} + \mathbf{e}_v \mathrm{rot}\ \mathbf{F}, \tag{3.13}$$

another equation (which we omit here as it is not needed further in this paper) can be obtained extracting the time-derivative from relation (3.12) and using Eqs. (3.1) and (3.2). A comparison of these two equations for η leads to a diagnostic relation

$$\Delta \left(l_e^2 \frac{\omega_0}{a} + \int_p^a \frac{\mathrm{d}p}{p^2} l_i^2 \omega \right) - \frac{\partial \omega}{\partial p} =$$

$$\frac{1}{f_0}(A_\eta + \mathbf{e}_v \mathrm{rot}\ \mathbf{F}) - \frac{l_e^2}{p_0} \Delta A_\xi - \frac{R}{f_0} \Delta \int_p^a \frac{\mathrm{d}p}{p} \left(A_T + \frac{W}{c_p} \right).$$

The omega-equation (3.8a) follows from here after applying the operator $(-p\partial/\partial p)$, while the boundary condition (3.8b) presents the obtained relation at the sea-level $p = a$. Eqs. (3.1), (3.2) and (3.8) perform the QG prognostic system of equations with temperature and GSP in the role of ruling fields. As the variable transformation $T, \xi \Leftrightarrow \eta$ is, according to (3.12), a one-to-one mapping, this system is equivalent to the QG model in variables $\eta - \omega$ consisting of Eqs. (3.8), (3.12) and (3.13). The main advantages of the system (3.1), (3.2), (3.8) in comparison with (3.8), (3.12), (3.13) is that it

1) exploits the prognostic fields T and ξ, which are the primary quantities obtained from synoptic observations;

2) is easier to solve, because it presents a system consisting of two prognostic and one diagnostic equation, while the alternative system consists of two diagnostic equations and one prognostic equation.

3) is easy to interpret.

The energy density for the system (3.1), (3.2), (3.8) is

$$E = \frac{1}{2}\left[\mathbf{v}_g^2 + R\frac{T^2}{T_i} + c_e^2\left(\frac{\xi}{a}\right)^2\right]. \tag{3.14}$$

A fraction of energy is located in the pressure deviations ξ – the free surface acts like an elastic membrane. As a consequence, the differential conservation law for energy may be compiled for the vertically averaged energy only

$$\frac{\partial \overline{E}}{\partial t} + \operatorname{div} \mathbf{J}_E = S_E, \tag{3.15a}$$

where

$$\mathbf{J}_E = \overline{\mathbf{v}_g E} + \overline{\mathbf{v}(\Phi_T + \Phi_b)}, \tag{3.15b}$$

$$S_E = \frac{\overline{RTW}}{c_p T_i} + \overline{\mathbf{v}_g \mathbf{F}}. \tag{3.15c}$$

The existence of the free boundary and the use of two prognostic equations in our system causes some differences in comparison with ordinary QG model in the potential vorticity treatment, too. Namely, two different potential vorticities exist simultaneously – the baroclinic vorticity Q and the barotropic vorticity K:

$$Q = \frac{1}{f_0}\Delta(\Phi_T + \Phi_b) + f - f_0\frac{\partial}{\partial p}\frac{pT}{T_i}, \tag{3.16a}$$

$$K = \frac{1}{f_0}\Delta(\overline{\Phi}_T + \Phi_b) + f - \frac{f_0}{c_e^2}\Phi_b. \tag{3.16b}$$

Q and K evolve according to the equations

$$\frac{\mathrm{d}_g}{\mathrm{d}t}Q - \operatorname{rot}\mathbf{F} = -\frac{\partial}{\partial p}f_0\frac{pW}{c_p T_i}, \tag{3.17a}$$

$$\frac{\mathrm{d}_g}{\mathrm{d}t}\overline{K} - \overline{\operatorname{rot}\mathbf{F}} = -\operatorname{div}\overline{\mathbf{v}'_g\eta'}. \tag{3.17b}$$

Here $\mathbf{v}'_g = \mathbf{v}_g - \overline{\mathbf{v}_g}$ and $\eta' = \eta - \overline{\eta}$ are the departures of the geostrophic wind and absolute vorticity from the vertical mean values. As it can be seen, Q becomes a conservative quantity in the absence of friction and diabatic heating, while the conservation of K takes place in the absence of friction and vertical fluctuations $\mathbf{v}'_g$ and η'. Note that K is not

the vertical mean of Q. In the principal plane, relations (3.16) and (3.17) can be used as the base system instead of Eqs. (3.1), (3.2) and (3.8) for the computation of the dynamics of the atmosphere. In this case, (3.16a) and (3.16b) must be considered as equations for temperature and GSP determination.

4. COMPARISON WITH THE ORDINARY QUASIGEOSTROPHIC MODEL

The obtained model differs from the ordinary QG model in the lower boundary treatment. In our model the lower boundary of the atmosphere is a free surface in the baric space, which evolves according to Eq. (3.2). In the common model the lower surface is fixed and, as a consequence, the evolutionary Eq. (3.2) is replaced by the condition

$$\omega|_{p=a} = 0. \tag{4.1}$$

Thus, the common model is grounded on the assumption that in Eq. (3.2) the individual time derivative of the GSP $\mathrm{d}_g\xi/\mathrm{d}t$ can be treated as a negligibly small quantity. In its nature this assumption expresses the hypothesis that the ground surface pressure field and (which is equivalent) the mass distribution in the atmosphere are adjusted to temperature and velocity fields. Approximation (4.1) is quite similar to the "rigid lid" approximation, often applied in ocean dynamics, and by analogy it may be called the "rigid bottom" approximation.

Assumption (4.1) is quite common among filtered models. For instance, in models which use the generalized z-co-ordinate [11]

$$z = z_0\left[1 - \left(\frac{p}{a}\right)^{\gamma}\right],$$

the boundary condition is

$$\dot{z} \equiv \frac{\mathrm{d}z}{\mathrm{d}t} = 0.$$

As $\dot{z} \sim \omega$, the last condition is equivalent to (4.1).

Changes, which appear in the QG model, if the "exact" Eq. (3.2) is replaced by the rigid bottom condition (4.1), can be characterized as follows:

1. The equations for ω (3.8a) and for η (3.13) remain the same including the expression for sources S (3.9);
2. The boundary condition (3.8b) is replaced by the rigid bottom condition (4.1);
3. In the case of the full model two alternative systems of equations are possible – equations for T, ξ, ω ((3.1), (3.2), (3.8a)) or for η, Φ, ω ((3.8a), (3.12), (3.13)). In the rigid bottom approximation only the second set is valid;
4. The GSP is not zero in the rigid bottom case, though, differently from

the full system, it cannot be calculated from an evolutional equation but using the diagnostic relation (3.12) only.

5. Energy density lacks the fraction, related to the free boundary deviations (compare with (3.14)):

$$E = \frac{1}{2}\left(\mathbf{v}_g^2 + R\frac{T^2}{T_i}\right).$$

6. The expression for K-vorticity (3.16b) modifies and coincides with the vertically averaged absolute vorticity:

$$K = \frac{1}{f_0}\Delta\,(\overline{\Phi_T} + \Phi_b) + f.$$

The Q-vorticity (3.16a) and Eqs. (3.17) remain the same.

To find out when the rigid bottom model is justified, it is neccessary to study the conditions when Eq. (3.2) may be replaced by condition (4.1). In the short-scale domain

$$\left| l_e^2 \Delta \right| \gg 1, \tag{4.2}$$

taking into account the definition of the term σ (3.10), the exact boundary condition (3.8b) may be approximately replaced by the relation

$$\omega_s = -A_\xi.$$

Together with Eq. (3.2) the condition $\partial\xi/\partial t = 0$ follows from here. This means that the GSP fluctuations will not be activated if they are absent at the initial moment. Therefore, the zero-condition (4.1) is approximately valid in the short scale domain, indeed.

To motivate the rigid bottom condition (4.1), often [5] an argument is used that typical values of ω in the middle atmosphere, say at a level p = 500 hPa, are much larger than those at the lower boundary. The easiest way to verify this argument is to model the vertical velocity ω according to Eq. (3.8) for typical simple model conditions. It is easy to solve (3.8) in the case of the constant stability parameter T_i using the Fourier transformation in horizontal co-ordinates $\mathbf{x} = (x, y)$. Let $\omega_k(p)$, $S_k(p)$ and $\sigma_k(p)$ be the Fourier coefficients of $\omega(\mathbf{x},p)$, $S(\mathbf{x},p)$ and $\sigma(\mathbf{x},p)$ (the time variable t is omitted), then the solution of Eq. (3.8) is

$$\omega_k = \frac{2a\sigma_k}{M_+}\left(\frac{p}{a}\right)^{(\alpha+1)/2} + \int_0^a q_k(p,p')\,S_k(p')\,\mathrm{d}p', \tag{4.3a}$$

$$q_k(p,p') = \frac{1}{\alpha}\left(\frac{p}{p'}\right)^{1/2}\begin{cases}\left(\dfrac{p}{p'}\right)^{\alpha/2} - \dfrac{M_-}{M_+}\left(\dfrac{pp'}{a^2}\right)^{\alpha/2}, & p' > p;\\[2ex] \left(\dfrac{p'}{p}\right)^{\alpha/2} - \dfrac{M_-}{M_+}\left(\dfrac{pp'}{a^2}\right)^{\alpha/2}, & p > p';\end{cases} \tag{4.3b}$$

$$\alpha = \sqrt{1 + 4l_i^2 k^2}, \tag{4.3c}$$

$$M_{\pm} = 1 + 2l_e^2 k^2 \pm \alpha, \qquad (4.3d)$$

and $k^2 = k_x^2 + k_y^2$.

Some profiles of ω_k/a are presented in Fig. 1 for $\sigma_k = 0$ and for singular sources of unit power $S = \delta(p - p_0)$ as functions of the argument p/a for waves with the scale $L\ (= 1/k) = l_i$ and $L = 2l_i$. Modelling is carried out in case l_i = 800 km, l_e = 2800 km, which assumes the model parameters

$$\varphi = 45°N, \quad T_0 = 280K, \quad T_i = 32K. \qquad (4.4)$$

The vertical velocity at the ground ω_0 consists of a considerable fraction of the maximum value of ω (which is reached at the level p_0) in the domain $L > 500$ km, which corresponds to the planetary-scale movements (wavelengths about 2000 km). This result is in good agreement with the observable space-scales of the GSP fluctuations.

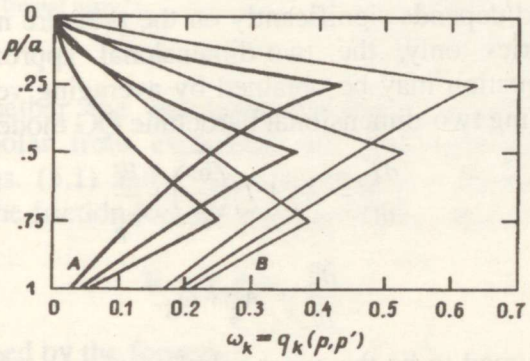

Fig. 1. Relative vertical velocity ω_k in the case of a singular unit source at the level p' = 250, 500, 750 hPa. *A* - 1/k = 800 km; *B* - 1/k = 1600 km.

As a consequence, we can conclude that the approximate boundary condition (4.1), which realizes the rigid bottom model in the QG framework, is valid for synoptic scale movements $L < 500$ km, while for planetary scales ($L > 500$ km) the "full" model with Eq. (3.2) and the boundary condition (3.8b) must be employed.

In the principal plane, the "full" model is more precise than the common one, because it does not utilize the additional rigid bottom approximation. Besides, it is more convenient to solve the evolutional equation for the GSP and temperature fields than to solve the evolutional equation for the absolute vorticity and, in addition, to solve at every time step the elliptical diagnostic Eq. (3.12) with respect to the GSP and temperature fields. And last, but not least: differently from the common QG model our system incorporates the shallow-water model as a special subcase. The shallow-water equations can be obtained, neglecting temperature fluctuations and considering the GSP evolution in accordance with Eq. (3.2) and with the omega Eq. (3.8).

5. THE ONE-LEVEL BAROCLINIC MODEL

The simplest model which incorporates baroclinic effects in the rigid bottom case is the two-level QG model [10]. In the presence of the free boundary the most simple baroclinic model can be represented by a one-level system. The one-level model follows if we assume that the temperature fluctuations T are independent of the pressure. The corresponding model is then presented by the two-dimensional fields $\xi(\mathbf{x},t)$ and $T(\mathbf{x},t)$.

Strictly speaking, the assumption of the two-dimensionality of T is not exactly consistent with Eq. (3.1) – from the assumption $\partial T/\partial p|_{t=0} = 0$ it does not follow the same for the successive moments, because the term ω/p depends to some degree on pressure. To get a closed two-dimensional model, an exact equation for temperature (3.1) must be replaced with an approximate one where all forcing terms are independent of the vertical co-ordinate.

Since ω/p is roughly constant in the wide pressure-range in the middle atmosphere and depends significantly on the pressure near the lower and upper boundaries only, the two-dimensional approximation for the temperature equation may be obtained by averaging vertically Eq. (3.1). Then the resulting two-dimensional baroclinic QG model will be

$$\frac{\partial T}{\partial t} = A_T + T_i\overline{\left(\frac{\omega}{p}\right)} + \frac{W}{c_p}, \tag{5.1}$$

$$\frac{\partial \xi}{\partial t} = A_\xi + \omega_S. \tag{5.2}$$

Here ω is assumed to be the exact solution of the problem (3.8), T_i is a constant typical for the troposphere, and W is the height-independent diabatic forcing. The temperature and GSP advections are

$$A_T = -\mathbf{v}_b \nabla T, \quad A_\xi = -\overline{\mathbf{v}}_T \nabla \xi. \tag{5.3}$$

where $\mathbf{v}_b$ and $\overline{\mathbf{v}}_T$ are the baric and vertically averaged thermal components of the geostrophic wind

$$\mathbf{v}_b = \frac{1}{f_0}\mathbf{e}_v \times \nabla \Phi_b = \frac{c_e^2}{af_0}\mathbf{e}_v \times \nabla \xi, \tag{5.4a}$$

$$\overline{\mathbf{v}}_T = \frac{1}{f_0}\mathbf{e}_v \times \nabla \overline{\Phi}_T = \frac{R}{f_0}\mathbf{e}_v \times \nabla T. \tag{5.4b}$$

Expressions (5.3) and (5.4) are exact in the case of the height-independent temperature.

Note that the temperature advection is caused by the baric wind, and the GSP advection is caused by the mean thermal wind. Such character of the advective interaction between temperature and GSP fields gives an explanation to the frontal instability and the polar front meandering. According to the classical model of the polar front [12], the surface highs

and lows are placed under the descending and ascending nodes of the temperature wave (Fig. 2). Causing the clockwise revolving of descending nodes and the contra-clockwise revolving of ascending nodes, they increase the amplitude of the frontal wave.

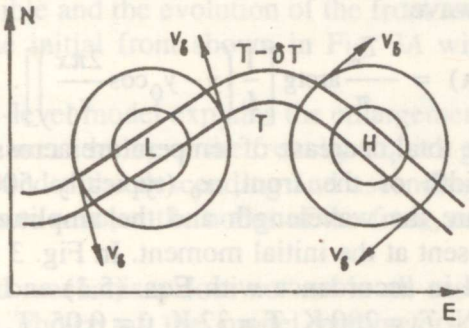

Fig. 2. Polar front and the corresponding baric field at the ground surface. Arrows show the baric winds. The baric winds are height-independent and try to increase the slopes of the descending and ascending nodes of the frontal wave.

To verify whether the one-level baroclinic model is capable of describing the polar front evolution, we have carried out numerical integration of Eqs. (5.1) and (5.2), assuming $W = 0$ and calculating ω from Eq. (4.3). The friction force $\mathbf{F}$ was modelled, using the relation

$$\mathbf{F} = f_0 \hat{F} (\mathbf{v}_g + \mathbf{v}_{fr}), \tag{5.5a}$$

where $\mathbf{v}_{fr}$ is defined by the formula

$$f_0 \mathbf{e}_v \times \mathbf{v}_{fr} = \mathbf{F} \tag{5.5b}$$

and

$$\hat{F} = \frac{\partial}{\partial p} \frac{p^2 \mu^2}{2} \frac{\partial}{\partial p}, \tag{5.5c}$$

$$\mu = h_1/h_0, \quad h_1 = \sqrt{2\kappa/f}, \quad h_0 = RT_0/g. \tag{5.5d}$$

Here κ is the turbulent friction coefficient ($\kappa = m^2/s$), h_1 is the boundary layer depth, h_0 – the height scale of the troposphere and the small parameter μ (at midlatitudes $\mu \approx 0.05$) presents the relative depth of the boundary layer. Relations (5.5a)–(5.5c) perform a linear equation for the friction forcing $\mathbf{F}$, which is easy to solve for the constant μ. The used friction model is consistent with the energy law (garantees the monotone dissipation of mechanical energy) and allows to model the friction force in the entire depth of the atmosphere. Of course, really the main friction forcing is located in the boundary layer, where it coincides in broad lines with the Ekman model. The main difference with the Ekman model is that in our case the boundary layer is baroclinic. The model, presented by (5.5a)–(5.5c), may be considered as an extension of the baroclinic boundary layer treatment [13–16] to the whole depth of the atmosphere.

The integration domain was $10^4 \times 10^4$ km, which was covered by a grid 64×64 points. The fast Fourier transform was used to compute spatial derivatives. For the integration in time the fourth-order Runge-Kutta scheme was used with the time step 1 hour. The polar front evolution was modelled in the beta-plane with the initial temperature disturbance in the form of a sinusoidal wave:

$$T(x) = -\frac{T_m}{\pi} \operatorname{arctg}\left[\frac{1}{L}\left(y - y_0 \cos\frac{2\pi x}{x_0}\right)\right]. \qquad (5.6)$$

Here $2T_m$ presents the total decrease of temperature across the front, $2L$ is the characteristic width of the front, x_0 (typically 5000 km) and y_0 (typically 100 km) are the wavelength and the amplitude of the initial wave. The GSP is absent at the initial moment. In Fig. 3 the evolution of the front is presented in accordance with Eqs. (5.1) and (5.2) for model parameters $\varphi = 60°$ N, $T_0 = 280$ K, $T_i = 32$ K, $\mu = 0.05$, $T_m = 10$ K, $L = 500$ km, $y_0 = 100$ km, $x_0 = 5000$ km. In Fig. 3*A* the initial front is shown, Fig. 3*B* presents the front after a four-day evolution and Fig. 3*C* – after an eight-day evolution. The evolution of the front and the corresponding development of the GSP field is quite realistic. The rise of mature ground

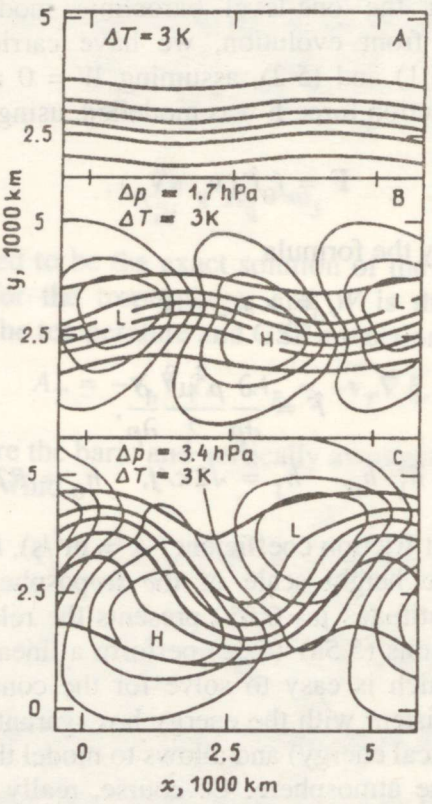

Fig. 3. The polar front and ground surface pressure field evolution according to the one-level baroclinic model. *A* -initial front; *B* - after 4-day evolution; *C* - after 8-day evolution.

cyclones and anticyclones takes about one week in our example. The maximum of the pressure fluctuations 12.8 hPa is reached on the eighth day, after which GSP begins to decrease steadily due to friction. If the GSP fluctuations are eliminated by replacing the equation for the GSP (5.2) by the relation $\xi = 0$, then the frontal meandering demonstrated in Fig. 3 becomes impossible and the evolution of the front reduces to the eastward translation of the initial front shown in Fig. 3*A* without changes in the wave amplitude.

Thus, the one-level model explains the enlargement of the amplitude of the wave and the meandering of the front by a quick generation of the GSP highs and lows under the descending and ascending nodes of the wave, which then starts to revolve the nodes of the front, enlarging the slopes of the wave.

The described mechanism does not act in all cases because it is quite sensitive to the choice of the model parameters. The front becomes unstable and begins to meander, if the temperature gradient at the front axis, T_m/L, is large enough and the friction is moderate ($\mu << 1$). For instance, the demonstrated model becomes stable if the temperature amplitude is reduced twice ($T_m = 5$ K instead of the used value 10 K). The friction decreasing ($\mu \Rightarrow 0$) has a double effect on the flow. Firstly, the growth rate of the GSP amplitude increases significantly. Secondly, the numeric integration scheme becomes unstable and some kind of short-scale turbulence is activated in the model. A significant stabilizing effect has the adding of the term $\sim y$ to the initial temperature profile (5.6). An explanation to this is that an additional uniform temperature gradient causes an additional thermal westerly wind, uniform in the y-direction and increasing with height, which tries to smear the initial wave (5.6) before the revolving mechanism is activated.

The general conclusion, which follows from the preliminary numeric integration of the one-level model, is that it gives a realistic description of the polar front meandering and that this model may be useful for the study of the baroclinic instability connected with the polar front and the polar jet-stream.

REFERENCES

1. Кибель И. А. Изв. АН СССР. Сер. географ., геофиз., 1940, 5, 627.
2. Charney, J. G. J. Meteorol., 1947, 4, 135-165.
3. Charney, J. G. J. Meteorol., 1949, **6**, 6, 371-385.
4. Обухов А. М. Изв. АН СССР. Сер. географ., геофиз., 1949, 13, 281.
5. Phillips, N. A. Rev. of Geophys., 1963, 1, 123-176.
6. Hoskins, B. J. J. Atm. Sci., 1975, **32**, 2, 233-242.
7. McWilliams, J. C., Gent, P. R. J. Atm. Sci., 1980, **37**, 8, 1657-1678.
8. Allen, J. S., Barth, J. A. and Newberger, P. A. J. Phys.Oceanogr., 1990, **20**, 7, 1017-1042.
9. Holton, J. R. An Introduction to Dynamic Meteorology. Academic Press, New York, 1979.
10. Haltiner, G. J., Williams, R. T. Numerical Prediction and Dynamic Meteorology. John Wiley & Sons, New York, 1980.

11. Hoskins, B. J., Bretherton, F. P. J. Atm. Sci., 1972, **29**, 1, 11-37.
12. Petterssen, S. Weather Analysis and Forecasting. Sec. edition, **1**, McGraw Hill, 1956.
13. MacKay, K. P. Boundary-Layer Meteorol., 1971, **2**, 161-168.
14. Wiin-Nielsen, A. Boundary-Layer Meteorol., 1974, **6**, 459- 476.
15. Arya, S. P. S., Wyngaard, J. C. J. Atm. Sci., 1975, **32**, 4, 767-778.
16. Bergström, H. J. Climate and Appl. Meteorol., 1986, **25**, 6, 813-824.

KVAASIGEOSTROOFILINE MUDEL TEMPERATUURI JA ALUSPINNA RÕHUGA BAASVÄLJADE ROLLIS

Rein RÕÕM

On tuletatud atmosfääri dünaamika kvaasigeostroofiline mudel, kus prognostilisteks baasvõrranditeks on temperatuurivälja ja aluspinna rõhuvälja evolutsioonivõrrandid. Mudeli muudab täielikult suletud süsteemiks vertikaalse kiiruse diagnostiline võrrand rõhukoordinaatides mittehomogeense ääretingimusega aluspinnal. Baasväljadena absoluutset pöörist, geopotentsiaali ja vertikaalkiirust kasutavast tavamudelist erineb uus mudel ääretingimuste üldisema käsitluse poolest. Saadud süsteemi integreerimine ja interpreteerimine on lihtsamad kui tavamudeli puhul. Tuletatud mudelvõrrandite lihtsaim erijuht on nn. ühekihiline barokliinne mudel, kus temperatuurivälja hälbed keskväärtusest ei sõltu kõrgusest atmosfääris. Nagu selgub toodud näidetest, kirjeldab ühekihiline mudel õigesti polaarfrondi evolutsiooni, sellega kaasnevat jugavoolu mittestatsionaarset looklemist ning madal- ja kõrgrõhkkondade moodustumist aluspinnal.

КВАЗИГЕОСТРОФИЧЕСКАЯ МОДЕЛЬ С ТЕМПЕРАТУРОЙ И ДАВЛЕНИЕМ НА ПОДСТИЛАЮЩЕЙ ПОВЕРХНОСТИ В РОЛИ ГЛАВНЫХ ПОЛЕЙ

Рейн РЫЫМ

Развита квазигеострофическая модель динамики атмосферы, использующая в роли основных уравнений прогностические уравнения для давления на подстилающей поверхности и для температуры. Систему замыкает диагностическое уравнение вертикальной скорости в изобарических координатах с неоднородным краевым условием на нижней границе. От обычной модели, использующей в качестве базовых полей абсолютную завихренность и вертикальную скорость, полученная модель отличается более общими краевыми условиями, простотой интегрирования и ясностью интерпретации. Наипростым частным случаем развитых уравнений является однослойная бароклинная

модель, в которой отклонения температуры от среднего значения не зависят от высоты в атмосфере. Примеры численного интегрирования однослойной модели показывают, что эта модель дает качественно правильное описание эволюции полярного фронта, сопутствующей меандрации струйного течения и генерации циклонов и антициклонов в нижней тропосфере.